124. Molecular Magnetism and Iron(II) Spin-State Equilibrium as Structural Probes in Heterodinuclear d–f Complexes

by **Claude Piguet*** and **Elisabeth Rivara-Minten**

Department of Inorganic, Analytical and Applied Chemistry, University of Geneva, 30, quai Ernest-Ansermet, CH–1211 Genève 4

and **Gérard Hopfgartner**

F. Hoffmann-La Roche Ltd., Pharma Division, Department of Drug Metabolism and Kinetics, Bioanalytical Section, CH–4002 Basel

and **Jean-Claude G. Bünzli**

Institute of Inorganic and Analytical Chemistry, University of Lausanne, BCH 1402, CH–1015 Lausanne

(7.VI.95)

$Fe(ClO_4)_2$ reacts with the segmental ligand 2-{6-[1-(3,5-dimethoxybenzyl)-1*H*-benzimidazol-2-yl]pyridin-2-yl}-1,1′-dimethyl-5,5′-methylene-2′-(5-methylpyridin-2-yl)bis[1*H*-benzimidazole] (L^2) in MeCN to give the diamagnetic deep violet complex $[Fe(L^2)_2]^{2+}$ where the metal is pseudo-octahedrally coordinated by two perpendicular tridentate binding units. When L^2 reacts with an equimolar mixture of $Ln(ClO_4)_3$ (Ln = La, Ce, Pr, Nd, Sm, Eu) and $Fe(ClO_4)_2$, electrospray-mass spectrometric, spectrophotometric, and ^{1}H-NMR data in MeCN show the selective formation of the deep red heterodinuclear C_3-cylindrical complexes $[LnFe(L^2)_3]^{5+}$ where the three ligands L^2 are wrapped about the metal-metal axis. Fe^{II} occupies the pseudo-octahedral capping site produced by the three bidentate units and Ln^{III} lies in the resulting 'facial' pseudo-tricapped trigonal prismatic site defined by the three remaining tridentate coordinating units. The heterodinuclear complexes $[LnFe(L^2)_3]^{5+}$ display spin-state equilibrium ($^1A \rightleftarrows {}^5T$) and thermochromism in MeCN between 243 and 333 K. Detailed ^{1}H-NMR, UV/VIS, and magnetic measurements in solution show that the partial spin-crossover behavior of $[LnFe(L^2)_3]^{5+}$ occurs for Ln = La–Eu with similar thermodynamic parameters ($\Delta H_{sc} = 20$–23 kJ·mol^{-1} and $\Delta S_{sc} = 55$–66 J·mol^{-1}·K^{-1}) indicating that the size of Ln^{III} has a negligible influence on the spin-state equilibrium. However, the smaller Ln^{III} ions have less affinity for the pseudo-tricapped trigonal prismatic coordination site in the heterodinuclear complexes as demonstrated by the partial decomplexation of $[YFe(L^2)_3]^{5+}$ to give $[Fe(L^2)_2]^{2+}$ and the absence of the heterodinuclear complex $[LuFe(L^2)_3]^{5+}$ under the same conditions. The crucial role played by the sterically demanding Fe^{II} in the assembly processes is discussed together with the use of the efficient combination of lanthanide probes with magnetic d-block probes for the design and investigation of luminescent and magnetic materials with controlled structural and physical properties. Photophysical measurements reveal that efficient ligand → metal and Eu → Fe energy transfers occur in $[EuFe(L^2)_3]^{5+}$ which strongly quench both the ligand and the Eu-centered luminescence.

Introduction. – The development of new molecular and supramolecular devices exhibiting controlled energy [1] and electron [2] transfers is currently a field of active research. Although trivalent lanthanides Ln^{III} are particularly suitable as luminescent probes [3], they are only rarely introduced into supramolecular architectures as a result of their versatile coordination behavior [4]. Highly preorganized cryptands [5] and podands [6] have been used to control the coordination sphere around Ln^{III}, but it was recently realized that less constrained ligands may also lead to well-defined lanthanide complexes. *E.g.*, Ln^{III} ions react with linear heterocyclic oligotridentate ligands such as L^3

and $\mathbf{L}^5$ to give triple-helical mononuclear $[Ln(\mathbf{L}^5)_3]^{3+}$ [7] and dinuclear $[Ln_2(\mathbf{L}^3)_3]^{6+}$ [8] complexes in which the metal ions occupy well protected pseudo-tricapped trigonal prismatic coordination sites [9]. Following this strategy, we have shown recently that related compounds can be produced by the assembly of the segmental ligand $\mathbf{L}^2$ with Ln^{III} and Zn^{II} which gives the heterodinuclear C_3-symmetrical complexes $[LnZn(\mathbf{L}^2)_3]^{5+}$ where Zn^{II} is pseudo-octahedrally coordinated by the three bidentate binding units and Ln^{III} nonacoordinated by the three remaining tridentate units [10]. In these complexes, Zn^{II} controls the coordination sphere around Ln^{III} and prevents *fac-mer*-isomerization of the C_3 pseudo-tricapped trigonal prismatic site. However, structural information relevant to the heterodinuclear complexes $[LnZn(\mathbf{L}^2)_3]^{5+}$ mainly comes from the tridentate units bound to Ln^{III} which behave as luminescent probes in the solid state (Ln = Eu) and NMR shift reagent in solution (Ln = Ce, Pr, Nd, Sm, Eu) [10]. It appears that the replacement of Zn^{II} by magnetically and spectroscopically active d-block metal ions would result in a deeper understanding of the assembly processes and of the structural properties of these hetero-

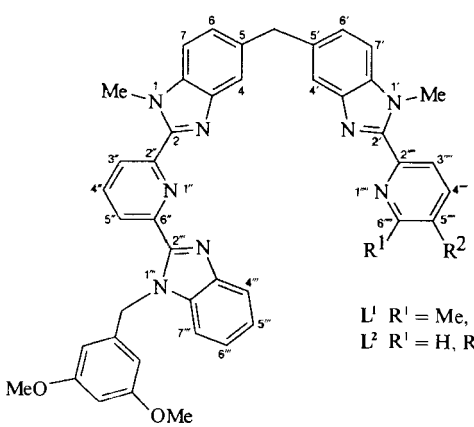

$\mathbf{L}^1$ R^1 = Me, R^2 = H
$\mathbf{L}^2$ R^1 = H, R^2 = Me

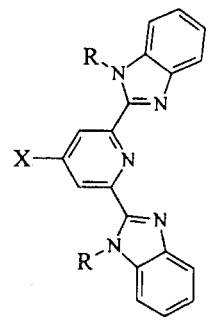

$\mathbf{L}^4$ R = H, X = H, Cl, OH
$\mathbf{L}^5$ R = Me, X = H
$\mathbf{L}^6$ R = $(MeO)_2C_6H_3CH_2$, X = H
$\mathbf{L}^7$ R = $(MeO)_2C_6H_3CH_2$, X = 4-R′-C_6H_4

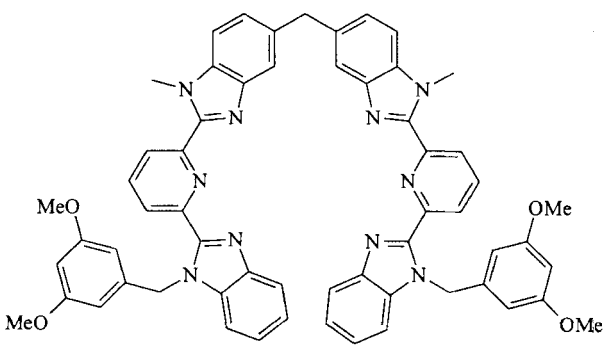

$\mathbf{L}^3$

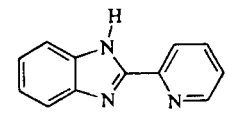

$\mathbf{L}^8$

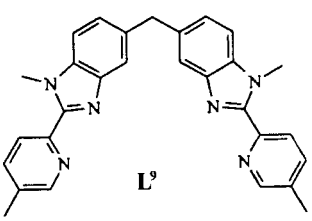

$\mathbf{L}^9$

dinuclear complexes in solution. Fe^{II} seems to be particularly suitable since its spin-state, spectroscopic and magnetic properties are very sensitive to the nature of coordinated aromatic heterocyclic binding units [11–16]. When Fe^{II} is pseudo-octahedrally coordinated by two tridentate units as in $[Fe(\mathbf{L}^n)_2]^{2+}$ (n = 5–7), it generally adopts a diamagnetic d^6 low-spin electronic configuration [11] [12], but spin-crossover behavior ($^1A \rightleftarrows {}^5T$) has been observed for $[Fe(\mathbf{L}^4)_2]^{2+}$ which possesses ligands with unsubstituted 1*H*-benzimidazole side arms whose NH groups are very sensitive to H-bonding [13] [14]. When Fe^{II} is pseudo-octahedrally coordinated by three bidendate heterocyclic units, a spin-crossover behavior is often observed both in solution and in the solid state [15], as reported for $[Fe(\mathbf{L}^8)_3]^{2+}$ [16]. We thus expect Fe^{II} to be a good candidate as a structural magnetic probe for monitoring the self-assembly of heterodinuclear d–f complexes with $\mathbf{L}^2$. Moreover, Fe^{II} may act as a receptor for intramolecular $Ln^{III} \rightarrow Fe^{II}$ energy-transfer processes [17].

In this paper, we report the detailed investigation of the assembly processes leading to the formation of the triple-helical heterodinuclear d–f complexes $[LnFe(\mathbf{L}^2)_3]^{5+}$ in MeCN together with their spin-state equilibrium properties in solution. Comparison of $[LnFe(\mathbf{L}^2)_3]^{5+}$ with the analogous complexes $[LnZn(\mathbf{L}^2)_3]^{5+}$ is also considered for the evaluation of Fe^{II} as a magnetic and spectroscopic structural probe.

Results and Discussion. – *Preliminary Remarks.* As reported for $[LnZn(\mathbf{L}^2)_3]^{5+}$ [10] and other heterodinuclear complexes [12], the detailed understanding of the assembly processes between $\mathbf{L}^2$, Ln^{III}, and Fe^{II} requires the preliminary investigations of the homonuclear precursors. We have previously shown that $\mathbf{L}^2$ reacts with $Ln(ClO_4)_3$ (Ln = La, Eu) in MeCN to give C_1-cylindrical head-to-tail dinuclear complexes $[Ln_2(\mathbf{L}^2)_3]^{6+}$ (structure **I**, *Fig. 1*) while Lu^{III} produces complicated mixtures of complexes [10]. To characterize the complexes formed between $\mathbf{L}^2$, Fe^{II}, and Ln^{III}, we used an efficient combination of electrospray-mass spectrometric (ES-MS), spectrophotometric, and ^{1}H-NMR titrations in solution [10] [12], followed by the detailed magnetic studies of the resulting supramolecular complexes using *Evans'* method in MeCN [18].

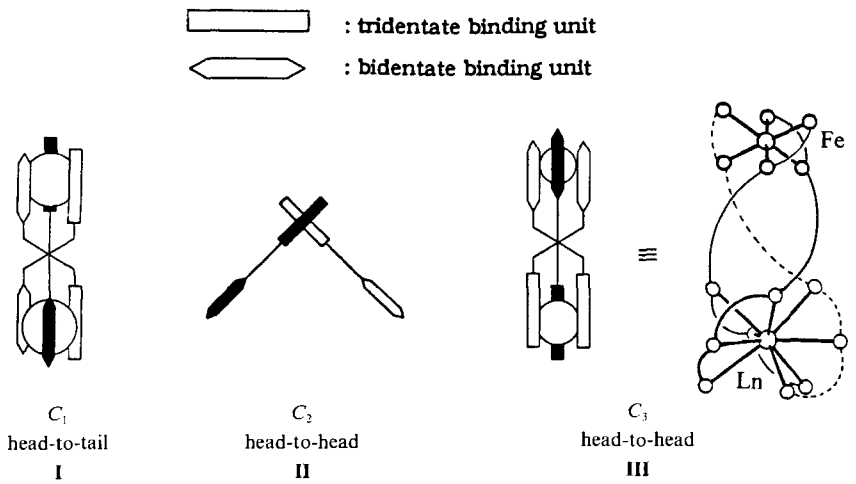

Fig. 1. *Different orientations of the bidentate and tridentate binding units*

Homodinuclear Complexes of L^2 *with* Fe^{II}. ES-MS Titrations of L^2 with $Fe(ClO_4)_2 \cdot 6 H_2O$ in MeCN show the exclusive formation of $[Fe(L^2)_2]^{2+}$ (*m/z* 738.8) for Fe/L^2 ratios in the range 0.1–0.5. In presence of a large excess of ligand, traces of $[Fe(L^2)_3]^{2+}$ are observed in the ES-MS (*Table 1*) as similarly reported for $[Zn(L^2)_3]^{2+}$ [10]. In presence of an excess of metal ($Fe/L^2 \geq 1.0$), $[Fe(L^2)_2]^{2+}$ still dominates the ES-MS, but significant peaks corresponding to $[Fe_2(L^2)_2]^{4+}$ (*m/z* 383.4) and its adduct ions with perchlorate,

Table 1. *Molecular Peaks of Complexes of* L^2 *and Adduct Ions Observed by ES-MS*

Metal	Cation	*m/z*[a])	Metal	Cation	*m/z*[a])
Fe^{II}	$[Fe(L^2)_3]^{2+}$	1094.2	Nd^{III}/Fe^{II}	$[NdFe(L^2)_3]^{5+}$	466.2
	$[Fe(L^2)_2]^{2+}$	738.8		$[NdFe(L^2)_3(ClO_4)]^{4+}$	607.8
	$[Fe_2(L^2)_2]^{4+}$	383.4		$[NdFe(L^2)_3(ClO_4)_2]^{3+}$	843.8
	$[Fe_2(L^2)_2(ClO_4)]^{3+}$	544.3		$[NdFe(L^2)_3(ClO_4)_3]^{2+}$	1315.5
	$[Fe_2(L^2)_2(ClO_4)_2]^{2+}$	866.2		$[Fe(L^2)_2]^{2+}$	738.8
	$[Fe_2(L^2)_2(ClO_4)_3]^{+}$	1831.8	Eu^{III}/Fe^{II}	$[EuFe(L^2)_3]^{5+}$	468.0
La^{III}/Fe^{II}	$[LaFe(L^2)_3]^{5+}$	465.4		$[EuFe(L^2)_3(ClO_4)]^{4+}$	610.8
	$[LaFe(L^2)_3(ClO_4)]^{4+}$	606.7		$[EuFe(L^2)_3(ClO_4)_2]^{3+}$	846.4
	$[LaFe(L^2)_3(ClO_4)_2]^{3+}$	842.1		$[EuFe(L^2)_3(ClO_4)_3]^{2+}$	1318.8
	$[LaFe(L^2)_3(ClO_4)_3]^{2+}$	1312.8		$[Fe(L^2)_2]^{2+}$	738.8
	$[Fe(L^2)_2]^{2+}$	738.8			

[a]) *m/z* Values given for the maximum of the peak.

$[Fe_2(L^2)_2(ClO_4)_i]^{(4-i)+}$ ($i = 1$–3, *Table 1*) [19], indicate the formation of a homodinuclear complex as reported for $[Fe_2(L^1)_2]^{4+}$ [12]. Spectrophotometric titrations under the same experimental conditions confirm these results and lead to a sharp end point for a Fe/L^2 ratio of 0.5 (isosbestic point at 30 770 cm^{-1} for Fe/L^2 in the range 0.1–0.5) and to a second smooth end point for Fe/L^2 1.0. Factor analysis [20] suggests the existence of two absorbing complexes, and the spectrophotometric data can be satisfactorily fitted to the equilibria of *Eqns. 1* and *2*.

$$Fe^{2+} + 2\ L^2 \rightleftarrows [Fe(L^2)_2]^{2+} \qquad \log(\beta_{12}^{Fe}) = 14.1(4) \tag{1}$$

$$2\ Fe^{2+} + 2\ L^2 \rightleftarrows [Fe_2(L^2)_2]^{4+} \qquad \log(\beta_{22}^{Fe}) = 20.0(8) \tag{2}$$

These results parallel those obtained with the analogous ligand L^1 which yields similar complexes $[Fe(L^1)_2]^{2+}$ ($\log(\beta_{12}^{Fe}) = 14.0(7)$) and $[Fe_2(L^1)_2]^{4+}$ (estimated $\log(\beta_{22}^{Fe}) = 17$) [12]. The larger stability found for the homodinuclear complex $[Fe_2(L^2)_2]^{4+}$ probably results from the shift of the Me group bound to C(6'''') of the pyridine ring in L^1 to C(5'''') in L^2 [10]. The electronic spectrum of $[Fe(L^2)_2]^{2+}$ displays the typical splitting of the $\pi \rightarrow \pi^*$ transitions (*Table 2*, *Fig. 2*) associated with the coordination of the tridentate binding unit to Fe^{II} as previously discussed for $[Fe(L^n)_2]^{2+}$ ($n = 5$–7) [11]. A strong metal-to-ligand charge-transfer (MLCT) band ($Fe^{II} \rightarrow \pi^*$) centered at 17 270 cm^{-1} (vibronic progression at 18 250 and 20 880 cm^{-1} [21], *Fig. 2*) is responsible for the deep violet color of the complex and corresponds to a low-spin Fe^{II} pseudo-octahedrally coordinated by two perpendicular tridentate units as found in $[Fe(L^6)_2]^{2+}$ (17 390 cm^{-1}) [11] and $[Fe(L^1)_2]^{2+}$ (17 270 cm^{-1}) [12]. Upon addition of a second equivalent of Fe^{II} to give $[Fe_2(L^2)_2]^{4+}$, the $\pi \rightarrow \pi^*$ transitions are further affected as similarly observed when going from $[Zn(L^2)_2]^{2+}$ to $[Zn_2(L^2)_2]^{4+}$

Table 2. *Electronic Spectral Data for* L^2 *in* $CHCl_3$ *and Its Complexes in MeCN*[a]) *and Electrochemical Reduction Potentials in MeCN + 0.1 M* $(Bu_4N)PF_6$[b]) *at 293 K*

	$\pi_{dmb} \rightarrow \pi^*$[c])	$\pi \rightarrow \pi^*$	MLCT	$E_{1/2}$	$E_p^a - E_p^c$
L^2	35490(28500, sh)	31450(55630)			
$[Fe(L^2)_2]^{2+}$	35715(62360, sh)	31750(97500)	20880(3560, sh)	0.82[d])	70
		28090(45340)	18250(7740, sh)	−1.06[e])	65
		26810(53310)	17270(9380)	−1.46[e])	65
$[Fe_2(L^2)_2]^{4+}$	35715(51910, sh)	31250(84520)	20450(4610, sh)		
		28490(76480, sh)	18485(5550)		
		27030(47970)	17330(4800, sh)		
$[LaFe(L^2)_3]^{5+}$	35715(60630, sh)	30550(88900)	18800(5070)	0.82[d])	65
		28410(66840, sh)		−1.03[e])	90
		26880(50860)		−1.32[e])	60
				−1.45[e])	75
				−1.61[e])	230
$[CeFe(L^2)_3]^{5+}$	35460(60050, sh)	30380(87800)	19050(5010)		
		28650(68060, sh)			
		27000(49940)			
$[PrFe(L^2)_3]^{5+}$	35430(59140, sh)	30300(87520)	18980(5050)		
		28650(66290, sh)			
		27250(50290)			
$[NdFe(L^2)_3]^{5+}$	35400(58800, sh)	30300(88600)	19010(5030)	0.84[d])	95
		28650(66400, sh)		−1.00[e])	80
		26900(49800)		−1.28[e])	70
				−1.42[e])	90
				−1.71[e])	250
$[SmFe(L^2)_3]^{5+}$	35340(62640, sh)	30450(87730)	18940(4980)		
		28820(66200, sh)			
		26880(49550)			
$[EuFe(L^2)_3]^{5+}$	35410(57600, sh)	30270(86100)	18870(5040)	0.83[d])	85
		28990(66100, sh)		−0.36	irrev
		27020(48500)		−1.01[e])	110
				−1.43[e])	75
				−1.69[e])	irrev

[a]) Energies are given for the maximum of the band envelope in cm^{-1} and ε's (in parentheses) in $M^{-1} \cdot cm^{-1}$; sh = shoulder.

[b]) Electrochemical potentials are given in V *vs.* SCE and $(E_p^a - E_p^c)$ in mV. Estimated error on $E_{1/2}$ is ±0.01 V.

[c]) Transitions centered on the 3,5-dimethoxyphenyl rings [10].

[d]) Reduction centered on metal.

[e]) Reduction centered on the ligand.

[10], which is attributed to the coordination of both bidentate and tridentate units of L^2 to the metal ions. The shape of the $Fe^{II} \rightarrow \pi^*$ MLCT transition is also strongly modified by the complexation of the second Fe^{II}, and the maximum of the band envelope is shifted by 1215 cm^{-1} toward higher energy, while reminiscence of the transition observed for $[Fe(L^2)_2]^{2+}$ is still observed as a shoulder at 17330 cm^{-1} (*Table 2*). This behavior suggests the coordination of both tridentate and bidentate units to Fe^{II} since the MLCT transitions of $[Fe(L^8)_3]^{2+}$ in solution is observed at higher energy (19230 cm^{-1}) [16].

^{1}H-NMR Titrations of L^2 (total ligand concentration $1.4 \cdot 10^{-2}$ M) by $Fe(ClO_4)_2 \cdot 6\,H_2O$ show the exclusive formation of $[Fe(L^2)_2]^{2+}$ for Fe^{II}/L^2 0.5. The ^{1}H-NMR spectrum

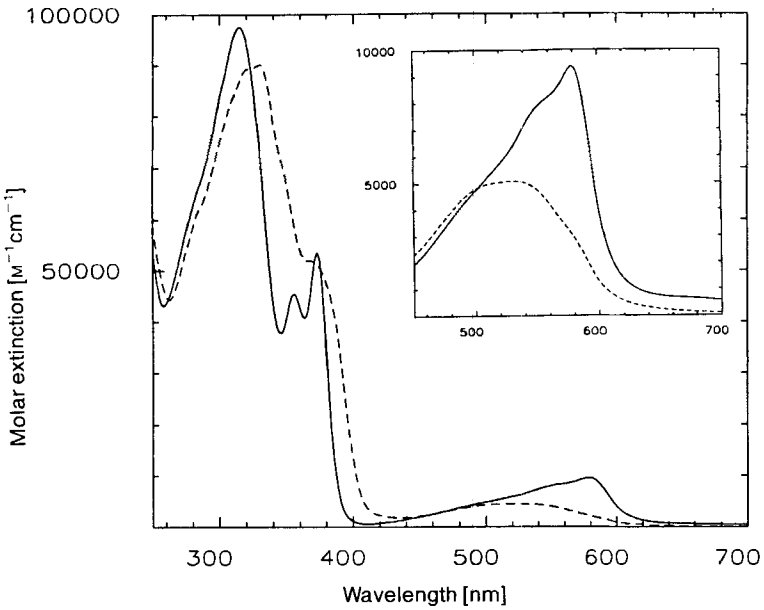

Fig. 2. *Absorption spectra of* $[Fe(L^2)_2]^{2+}$ (——) *and* $[LaFe(L^2)_3]^{5+}$ (---) *in MeCN at 293 K.* Total ligand concentration $6 \cdot 10^{-3}$ M.

Table 3. *^{1}H-NMR Shifts* (rel. to $SiMe_4$) *for Ligand* L^2 *in* $CDCl_3$ *and Its Complexes in* CD_3CN *at 294 K*

	Bidentate binding unit								
	Me–C(5'''')	Me–N(1')	H–C(6'''')	H–C(4'''')	H–C(3'''')	H–C(7')	H–C(6')	H–C(4')	CH_2–C(5')
L^2	2.39	4.21	8.49	7.61	8.22	7.30	7.18	7.66	4.26
$[Fe(L^2)_2]^{2+}$	2.46	4.36	8.61	7.79	8.34	7.42	6.85	7.21	3.76, 3.91
$[YFe(L^2)_3]^{5+}$	1.74	6.24	14.80	7.10	15.90	10.13	6.52	2.60	3.01, 3.60
$[LaFe(L^2)_3]^{5+}$	1.69	6.39	15.45	7.02	16.82	10.42	6.44	3.70	2.93, 3.69
$[CeFe(L^2)_3]^{5+}$	1.50	5.95	14.70	6.84	16.20	9.89	6.22	–0.77	2.78, 3.29
$[PrFe(L^2)_3]^{5+}$	1.25	6.06	15.00	6.52	16.30	8.81	7.00	0.60	2.63, 2.85
$[NdFe(L^2)_3]^{5+}$	1.43	5.96	15.00	6.72	16.24	9.92	6.13	–2.20	2.68, 3.14
$[SmFe(L^2)_3]^{5+}$	1.71	6.00	14.20	7.08	15.40	9.85	6.47	3.10	3.00, 3.58
$[EuFe(L^2)_3]^{5+}$	2.03	6.52	15.30	7.43	16.40	10.42	6.89	5.10	3.43, 4.18

	Tridentate binding unit											
	Me N(1)	H–C(4)	H–C(6)	H–C(7)	H–C(3'')	H–C(4'')	H–C(5'')	CH_2–N(1''')	H–C(7''')	H–C(6''')	H–C(5''')	H–C(4''')
L^2	3.66	7.69	7.22	7.22	8.29	8.00	8.42	5.90	7.30	7.40	7.20	7.85
$[Fe(L^2)_2]^{2+}$	4.12	5.49	7.23	7.31	8.46	8.38	8.57	5.78, 5.88	7.34	7.16	6.84	5.73
$[YFe(L^2)_3]^{5+}$	3.91	4.04	7.20	7.58	7.62	7.56	7.05	4.94, 5.62	7.35	7.18	6.60	6.60
$[LaFe(L^2)_3]^{5+}$	3.78	4.21	7.18	7.59	7.62	7.69	7.11	4.62, 5.38	7.36	7.16	6.59	6.95
$[CeFe(L^2)_3]^{5+}$	4.82	1.32	7.10	8.13	9.14	9.01	8.58	6.09, 6.68	8.12	7.34	6.30	3.09
$[PrFe(L^2)_3]^{5+}$	5.76	–6.43	5.92	9.75	11.26	10.38	10.68	7.85, 8.28	9.03	7.50	5.88	–1.50
$[NdFe(L^2)_3]^{5+}$	5.22	0.60	7.04	8.69	10.61	9.63	10.03	6.66, 7.47	8.70	7.33	6.14	1.80
$[SmFe(L^2)_3]^{5+}$	4.13	2.62	7.15	7.64	7.33	7.80	7.89	5.20, 5.78	7.47	7.21	6.55	5.87
$[EuFe(L^2)_3]^{5+}$	2.58	10.16	7.32	5.87	3.41	5.19	2.85	3.00, 3.16	5.49	7.10	7.19	11.92

displays 26 signals (CH_2–C(5′) and CH_2–N(1‴) are diastereotopic [22]) compatible with a C_2 point group for the complex as found for $[Zn(\mathbf{L}^2)_2]^{2+}$ [10] and $[Fe(\mathbf{L}^1)_2]^{2+}$ [12]. The signals of the protons of the bidentate units are only weakly altered by the coordination of Fe^{II} to $\mathbf{L}^2$, while the signals arising from the tridentate units are significantly modified (*Table 3*). The pyridine protons H–C(3″), H–C(4″), and H–C(5″) are shifted toward lower field ($\Delta\delta$ = 0.2–0.3 ppm), which is typical for N-coordination of the pyridine ring [23], and H–C(4) and H–C(4‴) are strongly shielded ($\Delta\delta$ = 2.20 and 2.12 ppm, resp.) demonstrating the perpendicular arrangement of the tridentate units which brings H–C(4) and H–C(4‴) of one ligand above the planes of the aromatic rings of the second ligand [10–12]. NOE's observed for Me–N(1)/H–C(3″) and CH_2–N(1‴)/H–C(5″) confirm the s-*cis*-,s-*cis*-conformation (N(1″) *cis* to N(3) and N(3‴)) of the tridentate units required by their coordination to Fe^{II} [10] [12], while the significant NOE for H–C(6⁗)/Me–N(1′) implies a s-*trans*-arrangement of the benzimidazole and pyridine rings (N(1⁗) *trans* to N(3′)) of the uncoordinated bidentate units. We conclude that $[Fe(\mathbf{L}^2)_2]^{2+}$ adopts the C_2 head-to-head structure **II** (*Fig. 1*) in solution as reported for the analogous complexes $[Fe(\mathbf{L}^1)_2]^{2+}$, $[Zn(\mathbf{L}^1)_2]^{2+}$ [12], and $[Zn(\mathbf{L}^2)_2]^{2+}$ [10] and resulting from the stronger chelate effect of the tridentate binding unit.

Susceptibility measurements using *Evans'* method [18] in MeCN between 243 and 333 K reveal that the weak molar paramagnetic susceptibility of Fe^{II} in $[Fe(\mathbf{L}^2)_2]^{2+}$ is temperature-independent and amounts to χ (Fe) = $2(1)\cdot 10^{-5}$ $cm^3\cdot mol^{-1}$. The small effective magnetic moment μ_{eff} = 0.2(1) BM at 293 K corresponds to a d^6 low-spin electronic configuration [24] with second-order *Zeeman* contributions [24] [25]. The large uncertainty on χ (Fe) arises from the small value of the paramagnetic susceptiblity as compared to the diamagnetic contribution of the ligands [14] used to correct the experimental data. $[Fe(\mathbf{L}^2)_2]^{2+}$ may thus be considered as essentially diamagnetic in solution, in agreement with ^{1}H-NMR and UV/VIS data.

Upon addition of $Fe(ClO_4)_2\cdot 6\,H_2O$ to a solution of $[Fe(\mathbf{L}^2)_2]^{2+}$ in MeCN, the ^{1}H-NMR signals become very broad and are of no more use. Magnetic measurements for Fe/$\mathbf{L}^2$ = 1.0 (total ligand concentration $1.4\cdot 10^{-2}$ M) confirm that the $[Fe_2(\mathbf{L}^2)_2]^{4+}$ complex evidenced by ES-MS and spectrophotometric data is paramagnetic in MeCN between 243 and 333 K. The corrected molar magnetic susceptibilities found for Fe^{II} are temperature-dependent: μ_{eff} varies from 1.8(1) BM per Fe-atom at 243 K to 2.60(8) at 333 K and lies between the expected values for low-spin (μ_{eff} = 0–0.5) and high-spin (μ_{eff} = 5.0–5.5) pseudo-octahedral or pseudo-tetrahedral Fe^{II} complexes with heterocyclic ligands [15] [16] [26]. However, a fit of the susceptibility data to a simple model taking into account the low-spin and high-spin species only failed, which leads us to suspect the presence of many structural isomers in solution.

Heterodinuclear Complexes of $\mathbf{L}^2$ *with* Fe^{II} *and* Ln^{III}. ES-MS Titrations of $\mathbf{L}^2$ by an equimolar mixture of $Fe(ClO_4)_2\cdot 6\,H_2O$ and $Ln(ClO_4)_3\cdot n\,H_2O$ (Ln = La, Nd, Eu) in MeCN reveal that only one heterodinuclear complex $[LnFe(\mathbf{L}^2)_3]^{5+}$ (and its adducts with perchlorate [19]) forms in solution for a $Fe^{II}/Ln^{III}/\mathbf{L}^2$ ratio of 1:1:3, together with significant quantities of $[Fe(\mathbf{L}^2)_2]^{2+}$ (*Table 1*). This suggests the existence of thermodynamic equilibria between mononuclear precursors and heterodinuclear complexes very similar to those reported for the assembly of $[LnZn(\mathbf{L}^2)_3]^{5+}$ [10] (*Fig. 3b*). Since the homodinuclear complexes $[Ln_2(\mathbf{L}^2)_3]^{6+}$ give weak ES-MS signals under these experimental conditions [10], one cannot rule out the presence of significant quantities of these complexes on the basis

of the ES-MS data. Spectrophotometric titrations of $\mathbf{L}^2$ by an equimolar mixture of $Fe(ClO_4)_2 \cdot 6\ H_2O$ and $Ln(ClO_4)_3 \cdot nH_2O$ (Ln = La, Eu) in MeCN (metal/$\mathbf{L}^2$ ratios in the range 0.1–2.0; [metal] = $[Ln^{III}] = [Fe^{II}]$) show an intricate variation of the molar extinction with a sharp end point for metal/$\mathbf{L}^2$ 0.3 followed by a monotonic evolution up to metal/$\mathbf{L}^2$ 1.0–1.2 (*Fig. 3a*). During these titrations, 10- to 15-min delays are necessary to reach thermodynamic equilibrium after each addition of metal, which contrasts with the

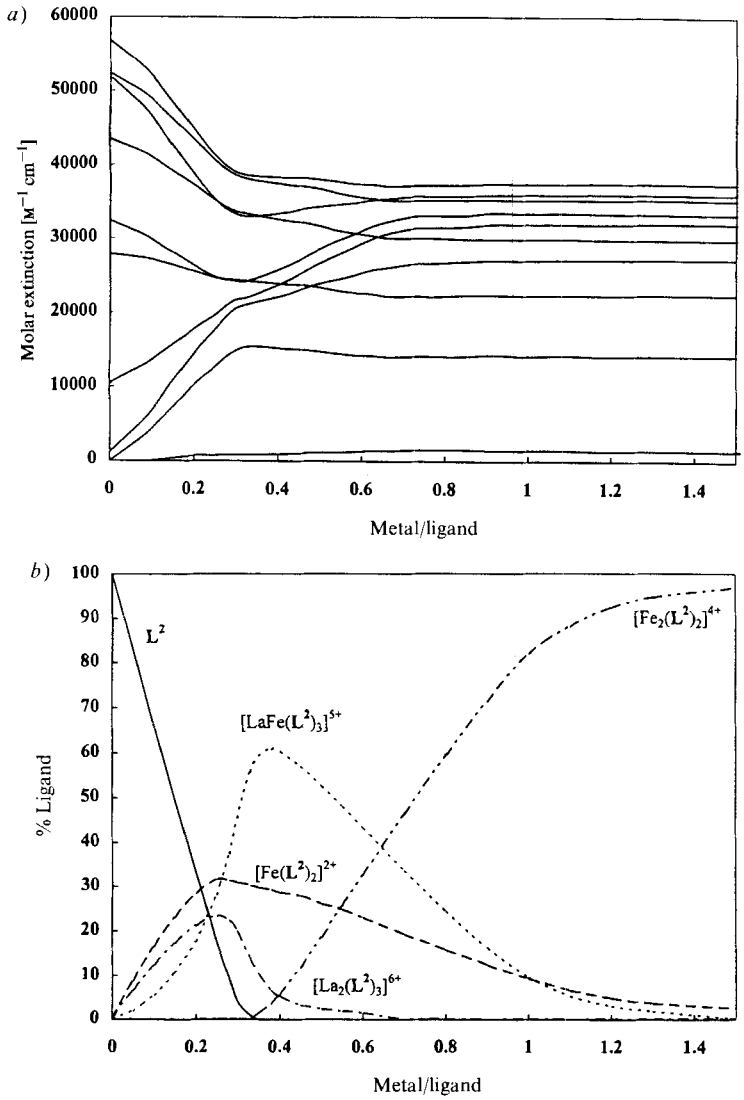

Fig. 3. a) *Variation of observed molar extinctions at 10 different wavelengths and* b) *corresponding calculated speciation of the ligand for the spectrophotometric titrations of* $\mathbf{L}^2$ *with an equimolar mixture of* $La(ClO_4)_3 \cdot 7\ H_2O$ *and* $Fe(ClO_4)_2 \cdot 6\ H_2O$ *in MeCN at 293 K.* Total ligand concentration 10^{-4} M; [metal] = $[La^{III}] = [Fe^{II}]$.

almost instantaneous formation of the corresponding Zn^{II} complexes [10]. This rather slow kinetics is expected, if inert d^6 low-spin Fe^{II} complexes are involved in the various equilibria [27]. The spectrophotometric data are fitted to the equilibria of *Eqns. 1–4* (Ln = La, Eu) with root-mean-square differences between calculated and observed molar extinctions of 0.003.

$$2\ Ln^{3+} + 3\ \mathbf{L}^2 \rightleftarrows [Ln_2(\mathbf{L}^2)_3]^{6+} \qquad \log(\beta_{23}^{La}) = 22.3(3)\ [10] \qquad (3)$$

$$\log(\beta_{23}^{Eu}) = 23.5(8)\ [10]$$

$$Ln^{3+} + Fe^{2+} + 3\ \mathbf{L}^2 \rightleftarrows [LnFe(\mathbf{L}^2)_3]^{5+} \qquad \log(\beta_{113}^{LaFe}) = 25.2(5) \qquad (4)$$

$$\log(\beta_{113}^{EuFe}) = 24.3(8)$$

The stability constants for $[LnFe(\mathbf{L}^2)_3]^{5+}$ (Ln = La, Eu) parallel those found for the analogous Zn^{II} complexes ($\log(\beta_{113}^{LnZn}) = 26.2(3)$ (Ln = La) and 25.3(4) (Ln = Eu)) [10]. However, the great similarity observed between the UV spectra of the complexes studied mean that the calculated β_{113}'s can only be considered as being mere estimations. The absorption spectra of $[LnFe(\mathbf{L}^2)_3]^{5+}$ (Ln = La, Ce, Pr, Nd, Sm, Eu; total ligand concentration $6 \cdot 10^{-3}$ M, > 80% of $[LnFe(\mathbf{L}^2)_3]^{5+}$ according to *Eqns. 1–4*) display a splitting of the $\pi \rightarrow \pi^*$ transitions similar to that found for $[LnZn(\mathbf{L}^2)_3]^{5+}$ [10] and typical of the coordination of both bidentate and tridentate units onto the metal ions [9–11]. A large and poorly structured MLCT transition ($Fe^{II} \rightarrow \pi^*$) [11] [14] [15] centered around 19000 cm^{-1} (*Table 2*, *Fig. 2*) is responsible for the deep red color of the Fe^{II} complexes. Compared to $[Fe(\mathbf{L}^2)_2]^{2+}$, the MLCT band of $[LnFe(\mathbf{L}^2)_3]^{5+}$ is significantly shifted toward higher energy (*ca.* 1700 cm^{-1}, *Fig. 2*) as found when going from $[Fe(terpy)_2]^{2+}$ (terpy = 2,2′:6′,2″-terpyridine; 18120 cm^{-1} [28]) to $[Fe(bipy)_3]^{2+}$ (bipy = 2,2′-bipyridine; 19160 cm^{-1} [21]) or $[Fe(\mathbf{L}^8)_3]^{2+}$ (19230 cm^{-1} [16]). This suggests that Fe^{II} is pseudo-octahedrally coordinated by the three bidentate binding units in $[LnFe(\mathbf{L}^2)_3]^{5+}$, and that the color change from violet to red observed when going from $[Fe(\mathbf{L}^2)_2]^{2+}$ to $[LnFe(\mathbf{L}^2)_3]^{5+}$ is associated with the transfer of the Fe^{II} ion from the tridentate units (structure **II**, *Fig. 1*) to the bidentate coordinating units. The intensity of the MLCT transitions of $[LnFe(\mathbf{L}^2)_3]^{5+}$ is strongly temperature-dependent (*Fig. 4*), leading to thermochromism and pointing to the presence of low-spin $\rightleftarrows$ high spin ($^1A \rightleftarrows {}^5T$) equilibria in MeCN solution [14] [15] [29], as reported for $[Fe(\mathbf{L}^8)_3]^{2+}$ [16] and other $[Fe(diimine)_3]^{2+}$ chromophores [15] [30]. The significant decrease of the molar extinction between 243 and 333 K corresponds to a decrease in the population of the low-spin state associated with the intense MLCT transition and is typical of partial spin-crossover behavior [15] [24] [30]. A quantitative analysis of the observed thermochromism will be discussed later. Unfortunately, the intense MLCT bands obscure any d–d transitions expected in this spectral range, preventing the determination of the ligand-field strength [15] [29].

For a total ligand concentration similar to the one used for ^{1}H-NMR titrations ($\geq 10^{-2}$ M), *Eqns. 1–4* predict that $[LnFe(\mathbf{L}^2)_3]^{5+}$ (Ln = La, Eu) is ten times more concentrated than any other species in solution. This is confirmed by the NMR spectra which reflect the formation of only one C_3-symmetrical complex with 26 signals (CH_2–C(5′) and CH_2–N(1‴) are diastereotopic) corresponding to $[LnFe(\mathbf{L}^2)_3]^{5+}$ (Ln = La, Ce, Pr, Nd, Sm, Eu; *Fig. 5*) as reported for $[LnZn(\mathbf{L}^2)_3]^{5+}$ (Ln = La–Lu) [10]. The short electronic relaxation times of lanthanides La–Eu [31] produce little line broadening of the ^{1}H-NMR

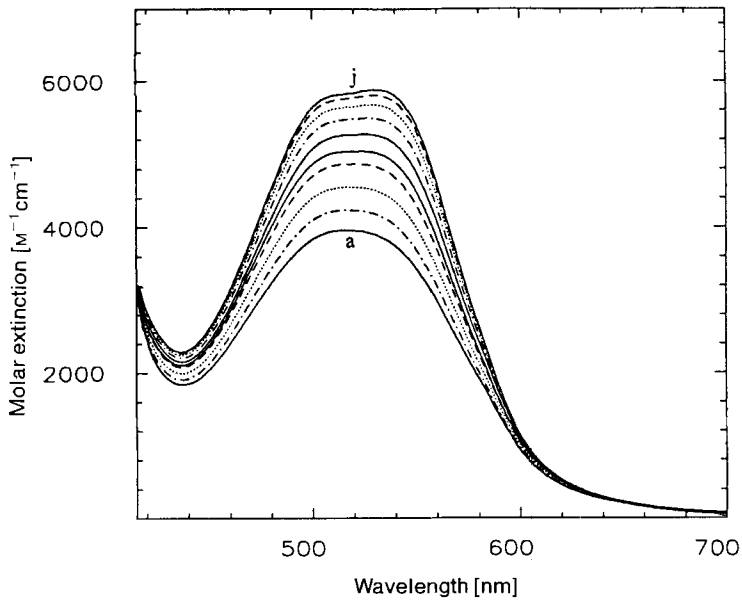

Fig. 4. *VIS Spectra of* $[NdFe(L^2)_3]^{5+}$ *in MeCN at stepwise decreasing temperatures* (ΔT = 10 K) *between 333 K* (a) *and 243 K* (j). Total ligand concentration $6 \cdot 10^{-3}$ M.

signals and allow reliable NOEDIF, 2D-COSY, and 2D-NOESY measurements leading to the assignments given in *Table 3*. Intra- and interstrand NOE's observed for $[LnFe(L^2)_3]^{5+}$ (Ln = La–Eu) strictly parallel those found for $[LnZn(L^2)_3]^{5+}$ [10] demonstrating that the Fe^{II} complexes adopt a triple-helical structure in solution with the three ligands L^2 wrapped around the C_3 axis defined by the metal ions. *E.g.*, intrastrand NOE's for H–C(3‴)/Me–N(1′), H–C(3″)/Me–N(1), and H–C(5″)/CH_2–N(1‴) imply s-*cis*-arrangements of the pyridine and benzimidazole rings within each coordinating unit resulting from its complexation to the metal ions while the particular NOE map of the protons of the 'diphenylmethane' spacer (observed NOE's: CH_a–C(5′)/H–C(4), CH_a–C(5′)/H–C(6′), CH_b–C(5′)/H–C(4′), CH_b–C(5′)/H–C(6), and H–C(4′)/H–C(4)) corresponds to the helical wrapping of the ligand [10] [12]. Weaker interstrand NOE's (Me–N(1)/CH_2–N(1‴), Me–N(1)/H–C(6′), and Me–N(1′)/H–C(6)) demonstrate that the three ligands L^2 are closely packed along the C_3 axis in agreement with the proposed triple-helical structure. For a given lanthanide, the δ(H)'s of the tridentate binding units are comparable for the two series of complexes $[LnFe(L^2)_3]^{5+}$ and $[LnZn(L^2)_3]^{5+}$ (Ln = La–Eu) (*Table 3* and [10]), *i.e.*, similar paramagnetic induced shifts are experienced by these protons. H–C(4) and H–C(4‴) are of particular interest, since they point toward the lanthanide in $[LnZn(L^2)_3]^{5+}$ leading to strong paramagnetic dipolar contributions to the observed chemical shifts [10]. *Bleaney*'s dipolar coefficients of the Ln^{III} ions point to a similar behavior for $[LnFe(L^2)_3]^{5+}$: H–C(4) and H–C(4‴) are strongly shielded for Ln = Ce, Pr, Nd, Sm (negative coefficients) and deshielded for Ln = Eu (positive coefficient, *cf. Table 3*) [32]. We conclude that the heterodinuclear complexes $[LnFe(L^2)_3]^{5+}$ adopt the triple-helical structure **III** in solution (*Fig. 1*) as previously established for the

analogous Zn^{II} complexes [10], where the lanthanide ion occupies the pseudo-tricapped trigonal prismatic coordination site produced by the three wrapped tridentate binding units of L^2 while Fe^{II} lies in the pseudo-octahedral site defined by the three bidentate units.

However, the ^{1}H-NMR signals of the bidentate units are completely different for $[LnFe(L^2)_3]^{5+}$ compared to $[LnZn(L^2)_3]^{5+}$: H–C(6''''), H–C(3''''), and Me–N(1') give broad and highly temperature-dependent signals at surprisingly low field (*Table 3*, *Fig. 5*). At 243 K, the ^{1}H-NMR spectra of the $[LnFe(L^2)_3]^{5+}$ complexes are very similar to those found for the analogous Zn^{II} complexes [10], in agreement with the conclusion that Fe^{II} is

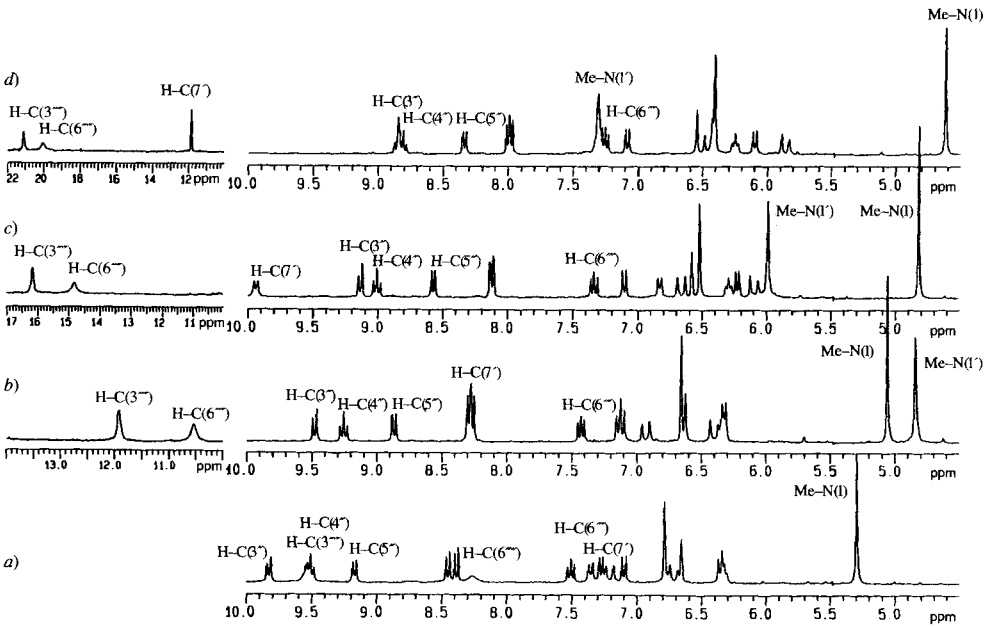

Fig. 5. *^{1}H-NMR Spectra of $[CeFe(L^2)_3]^{5+}$ at* a) *253 K*, b) *273 K*, c) *293 K, and* d) *303 K in CD_3CN*. Total ligand concentration $2.25 \cdot 10^{-2}$ M.

Table 4. *^{1}H-Longitudinal Relaxation Times (T_1[s]) for L^2 in $CDCl_3$ and Selected Complexes in CD_3CN at 294 K*

	Bidentate binding unit								
	Me–C(5'''')	Me–N(1')	H–C(6'''')	H–C(4'''')	H–C(3'''')	H–C(7')	H–C(6')	H–C(4')	CH_2–C(5')
L^2	0.78	1.09	3.03	1.60	2.11	1.05	1.38	2.10	0.36
$[Fe(L^2)_2]^{2+}$	0.71	0.68	2.02	1.23	1.16	0.87	0.79	1.08	0.30, 0.32
$[LaZn(L^2)_3]^{5+}$	0.71	0.56	1.35	1.20	0.80	0.84	0.61	1.67	0.21, 0.30
$[LaFe(L^2)_3]^{5+}$	0.16	0.31	0.33	0.30	0.20	0.50	0.35	0.52	0.18, 0.18

	Tridentate binding unit											
	Me–N(1)	H–C(4)	H–C(6)	H–C(7)	H–C(3'')	H–C(4'')	H–C(5'')	CH_2–N(1''')	H–C(7''')	H–C(6''')	H–C(5''')	H–C(4''')
L^2	0.78	1.83	1.31	1.06	1.78	1.00	1.82	0.31	1.07	1.03	1.06	1.99
$[Fe(L^2)_2]^{2+}$	0.47	0.45	0.73	0.78	0.55	0.70	0.47	0.20, 0.24	0.74	0.79	0.79	0.39
$[LaZn(L^2)_3]^{5+}$	0.46	1.62	0.76	0.82	0.75	0.78	0.73	0.21, 0.21	0.83	0.87	0.88	1.40
$[LaFe(L^2)_3]^{5+}$	0.40	0.50	0.50	0.55	0.68	0.65	0.51	0.20, 0.30	0.67	0.80	0.79	1.04

mainly diamagnetic at low temperature. As the temperature is increased, the appearance of an average paramagnetism is expected, if Fe^{II} displays a fast spin-state equilibrium $^1A \rightleftarrows {}^5T$ on the NMR time scale [15] [29]. This is confirmed by the significant decrease of the longitudinal relaxation times T_1 (Ln = La, *Table 4*) resulting from the coupling between the ^1H nuclear magnetic moments and the electronic magnetic moments of high-spin Fe^{II} [33]. Detailed analyses of the temperature-dependent ^1H-NMR spectra of $[LnFe(\mathbf{L}^2)_3]^{5+}$ and $[LnZn(\mathbf{L}^2)_3]^{5+}$ (Ln = La–Eu) in the range 243–333 K show that these complexes are the only species observed in solution and that the C_3 triple-helical structure **III** (*Fig. 1*) is maintained at all temperatures. No significant decomplexation nor the formation of other species is detected for total ligand concentrations in the range $1.4–2.5 \cdot 10^{-2}$ M. The addition of an excess of ligand induces the expected shift in the distribution of the various complexes (*Fig. 3b*); the well resolved spectrum found for free $\mathbf{L}^2$ indicates that potential ligand exchanges are slow on the NMR time scale.

For Ln = Y^{III}, a complicated ^1H-NMR spectrum is observed for a Y/Fe/$\mathbf{L}^2$ ratio 1:1:3 and corresponds to a *ca.* 55:45 mixture of $[Fe(\mathbf{L}^2)_2]^{2+}$ and $[YFe(\mathbf{L}^2)_3]^{5+}$, as estimated by integration of the ^1H-NMR signals. Other weak signals probably arise from diamagnetic Y^{III} complexes [10]. When $\mathbf{L}^2$ is titrated by Lu^{III} and Fe^{II}, the ^1H-NMR spectra contain sharp signals from $[Fe(\mathbf{L}^2)_2]^{2+}$ and poorly defined signals from diamagnetic Lu^{III} complexes [10], but no trace of $[LuFe(\mathbf{L}^2)_3]^{5+}$ is detected. The quantitative formation of the C_3-heterodinuclear complexes $[LnFe(\mathbf{L}^2)_3]^{5+}$ in solution is thus limited to the larger lanthanide ions (Ln = La–Eu) while the analogous Zn^{II} complexes are obtained with the complete lanthanide series [10]. This points out the sensitivity of the self-assembly processes to minor structural changes, since low-spin Fe^{II} (ionic radius: 0.61 Å [34]) is 18% smaller than Zn^{II} (0.74 Å [34]), and Y^{III} is only 4% smaller than Eu^{III} [4].

Slow diffusion of Et_2O into concentrated MeCN solutions of $[LnFe(\mathbf{L}^2)_3]^{5+}$ allows the almost quantitative isolation of deep red powders whose elemental analyses correspond to $[LnFe(\mathbf{L}^2)_3](ClO_4)_5 \cdot 8\,H_2O$ (Ln = La, **1**; Ln = Nd, **2**; Ln = Eu, **3**). These compounds are readily soluble in MeCN and give spectra (UV/VIS, ES-MS, ^1H-NMR) identical to those obtained for $[LnFe(\mathbf{L}^2)_3]^{5+}$ formed *in situ*, but we were unable to obtain crystals suitable for X-ray diffraction studies. Complexes **1**–**3** are oxidized on a Pt-disk electrode in a quasi-reversible monoelectronic wave at $E_{1/2} = 0.82–0.84$ V *vs.* SCE in MeCN + 0.1 M $(Bu_4N)PF_6$ (Fe^{III}/Fe^{II}, $E_p^a–E_p^c \approx 80$ mV, *Table 2*). This behavior parallels that of $[Fe(bipy)_3](ClO_4)_2$ ($E_{1/2} = 0.79$ V, $E_p^a–E_p^c = 70$ mV) [35], but is not typical of $[Fe(diimine)_3]^{2+}$ chromophores since $[Fe(triimine)_2]^{2+}$ complexes such as $[Fe(\mathbf{L}^1)_2]^{2+}$ ($E_{1/2} = 0.83$ V, $E_p^a–E_p^c = 70$ mV [12]) and $[Fe(\mathbf{L}^2)_2]^{2+}$ ($E_{1/2} = 0.82$ V, $E_p^a–E_p^c = 65$ mV) display similar oxidation waves. In addition, the cyclic voltammograms of $[Fe(\mathbf{L}^2)_2]^{2+}$ and $[LnFe(\mathbf{L}^2)_3]^{5+}$ (Ln = La, Nd), display several other waves (*Table 2*) corresponding to the successive reduction of each coordinated unit [36], but a precise interpretation is not possible. For Ln = Eu, another cathodic behavior is observed which is probably associated with the reduction of Eu^{III} into Eu^{II} [4].

Spin-State Equilibria of the Heterodinuclear Complexes [LnFe($\mathbf{L}^2$)$_3$]$^{5+}$ (Ln = La–Eu) *in MeCN.* The $[Fe(diimine)_3]^{2+}$ chromophores often display low-spin $\rightleftarrows$ high-spin equilibria (*Eqn. 5*) resulting from a ligand-field strength comparable to the mean spin-pairing energy [15] [29] [30]. This leads to thermal spin-crossover transitions, as reported for $[Fe(\mathbf{L}^8)_3]^{2+}$ and other analogous α,α′-diimine ligands [16] [30].

$$^1A\,(S = 0) \rightleftarrows {}^5T\,(S = 2) \quad \log(K_{sc}) \tag{5}$$

The temperature-dependent $Fe^{II} \rightarrow \pi^*$ MLCT transition and ^{1}H-NMR spectra of $[LnFe(L^2)_3]^{5+}$ (Ln = La–Eu) are typical of such equilibria [15] [29] and confirm the existence of a partial spin-crossover behavior in MeCN, which is not surprising, since Fe^{II} is pseudo-octahedrally coordinated by three bidentate units analogous to L^8 [16]. A detailed investigation of *Equilibrium 5* requires the direct determination of magnetic moments over a sufficient temperature range using *Evans'* method [18] adapted to superconducting NMR magnets [37]. Moreover, a reliable value for the diamagnetic contribution of the ligands and counter anions is needed, since this contribution is of the same order of magnitude as the paramagnetic susceptibility in large molecules [38]. Finally, a detailed knowledge of the paramagnetism associated with Ln^{III} ions is also required to interpret the magnetic data of the heterodinuclear complexes $[LnFe(L^2)_3]^{5+}$ (Ln = Ce–Eu).

The paramagnetic moments of Ln^{III} in $[LnZn(L^2)_3]^{5+}$ and the total paramagnetic moments of Ln^{III} and Fe^{II} in $[LnFe(L^2)_3]^{5+}$ in MeCN (Ln = La–Eu), calculated from measured susceptibilities corrected for diamagnetism (see *Exper. Part*), are given in *Table 5* and *Fig. 6*. The Ln^{III} ions in $[LnZn(L^2)_3]^{5+}$ follow a *Curie* behavior, within experimental error. Their effective magnetic moments are close to those expected for the free ions, μ_{eff} = 2.53, 3.58, 3.62, 1.80, and 3.35 BM for Ce, Pr, Nd, Sm, and Eu, respectively [24]. Since La^{III} is diamagnetic, the μ_{eff} (Fe) values reported for $[LaFe(L^2)_3]^{5+}$ point to a non-*Curie* behavior. For the other heterodinuclear complexes $[LnFe(L^2)_3]^{5+}$ with paramagnetic Ln^{III} ions, the determination of the magnetic behavior of Fe^{II} requires the separation of the contribution of the two metal ions. As a result of the ineffective overlap of the f-orbitals with the orbitals of the ligands or of the d-block metal ion [39], the isotropic interaction J between d and f metal ions in heteronuclear complexes is weak ($J < 10$ cm^{-1}) [40]. It may be neglected for the complexes $[LnFe(L^2)_3]^{5+}$ in solution, since there is no short-distance bridging ligand (the Ln–Fe distance estimated from the X-ray crystal structures of $[Eu_2(L^3)_3](ClO_4)_6$ [41] and $[Co_2(L^9)_3](ClO_4)_4$ [42] is 8–9 Å), and since $kT \gg |J|$ for the temperature range accessible in MeCN (243–333 K). We thus consider Fe^{II} and Ln^{III} as being two independent paramagnetic centers, as recently reported for heterodinuclear LnCu complexes [43]. The Ln^{III} paramagnetic moments are taken from

Table 5. *Effective Total Magnetic Moments* μ_{eff} [BM][a]) *for* $[LnFe(L^2)_3](ClO_4)_5$ *and* $[LnZn(L^2)_3](ClO_4)_5$ *at Different Temperatures in MeCN*

Metals	243 K	253 K	263 K	273 K	283 K	293 K	303 K	313 K	323 K	333 K
LaFe	0.98	1.19	1.37	1.59	1.81	2.04	2.28	2.56	2.82	3.05
CeFe	2.73	2.79	2.87	2.97	3.08	3.26	3.43	3.64	3.87	4.12
PrFe	3.65	3.68	3.74	3.79	3.89	4.01	4.13	4.30	4.47	4.66
NdFe	3.45	3.49	3.56	3.63	3.72	3.85	3.97	4.14	4.32	4.49
SmFe	1.75	1.86	1.95	2.11	2.29	2.45	2.64	2.91	3.17	3.43
EuFe	3.41	3.46	3.54	3.62	3.72	3.86	3.98	4.16	4.37	4.54
CeZn	2.54	2.54	2.53	2.52	2.51	2.50	2.50	2.47	2.45	2.46
PrZn	3.53	3.52	3.49	3.49	3.47	3.47	3.47	3.46	3.42	3.41
NdZn	3.33	3.31	3.32	3.33	3.33	3.32	3.32	3.32	3.31	3.30
SmZn	1.42	1.43	1.44	1.45	1.46	1.47	1.48	1.49	1.50	1.51
EuZn	3.30	3.29	3.31	3.32	3.33	3.32	3.34	3.32	3.33	3.32

[a]) μ_{eff} are corrected for diamagnetic contributions (see text). Estimated error is typically ±0.05 BM.

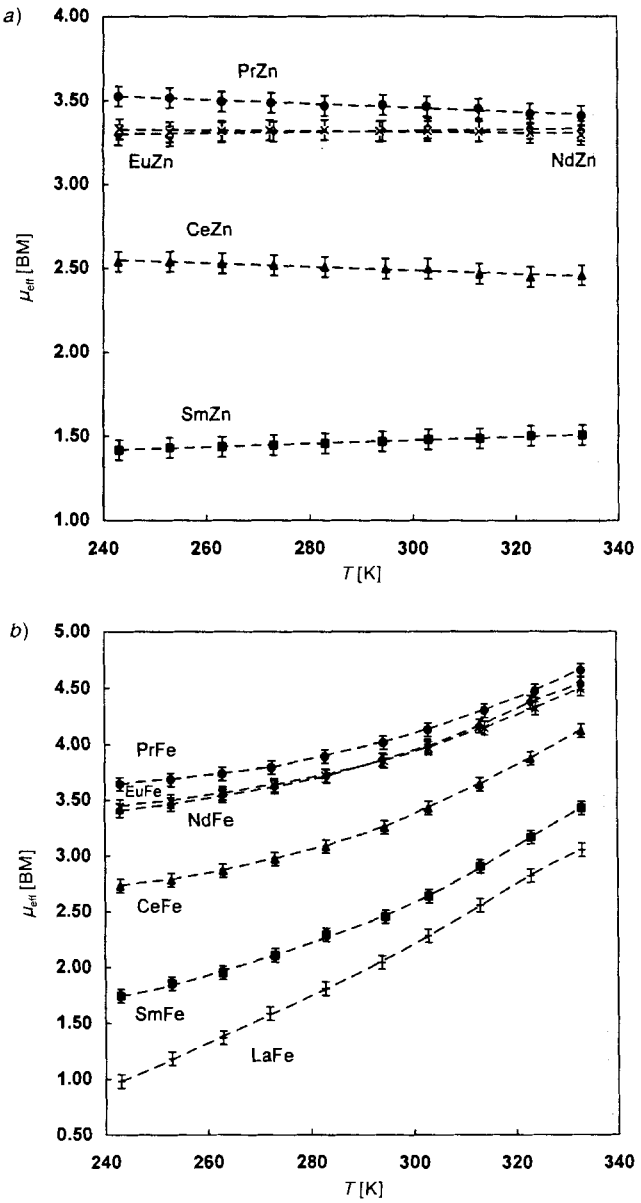

Fig. 6. *Corrected effective total magnetic moments* (μ_{eff}) vs. *temperature for* a) *[LnZn(*L^2*)$_3$]$^{5+}$* (Ln = Ce, Pr, Nd. Sm, Eu) *and* b) *[LnFe(*L^2*)$_3$]$^{5+}$* (Ln = La, Ce, Pr, Nd, Sm, Eu) *in MeCN*

the data determined for $[LnZn(L^2)_3]^{5+}$. The magnetic moments of Fe^{II} in $[LnFe(L^2)_3]^{5+}$ are consequently calculated according to *Eqn. 6*.

$$\mu^2_{eff}(Fe) = \mu^2_{eff}(LnFe) - \mu^2_{eff}(LnZn) \quad (6)$$

These moments are reported in *Table 6* and *Fig. 7a* and display a non-*Curie* behavior similar to that of $[LaFe(L^2)_3]^{5+}$. At all temperatures, the observed magnetic moments of

Table 6. *Effective Magnetic Moments* μ_{eff} [BM] *of* Fe^{II} *for* $[LnFe(L^2)_3](ClO_4)_5$ *and Calculated Mole Fractions* x_{hs} *of High-Spin* Fe^{II} *at Different Temperatures in MeCN*

Metals		243 K	253 K	263 K	273 K	283 K	293 K	303 K	313 K	323 K	333 K
LaFe	μ_{eff}	0.98	1.19	1.37	1.59	1.81	2.04	2.28	2.56	2.82	3.05
	x_{hs}	0.04	0.05	0.07	0.10	0.13	0.16	0.21	0.26	0.32	0.37
CeFe	μ_{eff}	0.98	1.15	1.35	1.58	1.79	2.08	2.35	2.67	2.98	3.28
	x_{hs}	0.04	0.05	0.07	0.10	0.13	0.17	0.22	0.28	0.35	0.43
PrFe	μ_{eff}	0.92	1.10	1.32	1.49	1.77	2.01	2.24	2.55	2.87	3.17
	x_{hs}	0.03	0.05	0.07	0.09	0.12	0.16	0.20	0.26	0.33	0.40
NdFe	μ_{eff}	0.89	1.10	1.29	1.49	1.67	1.99	2.17	2.47	2.76	3.05
	x_{hs}	0.03	0.05	0.06	0.08	0.11	0.16	0.19	0.24	0.30	0.37
SmFe	μ_{eff}	1.02	1.18	1.32	1.53	1.77	1.96	2.18	2.50	2.79	3.08
	x_{hs}	0.04	0.05	0.07	0.09	0.12	0.15	0.19	0.25	0.31	0.38
EuFe	μ_{eff}	0.86	1.08	1.24	1.45	1.65	1.97	2.17	2.51	2.83	3.10
	x_{hs}	0.03	0.04	0.06	0.08	0.11	0.15	0.19	0.25	0.32	0.38

Fe^{II} fall between the pure low-spin ($S = 0$, $\mu_{eff} = 0$–0.5 BM) and the pure high-spin limit ($S = 2$, $\mu_{eff} = 5.0$–5.5 BM) found for hexacoordinated Fe^{II} complexes [15] [30] [44]. The observed decrease of μ_{eff} at low temperature is similar to the one found for other solution-phase Fe^{II} spin-equilibrium processes [15] [24], and this, along with absorption and ^{1}H-NMR spectra, confirms the existence of the equilibrium of *Eqn. 5* for the Fe^{II} complexes. Assuming that no intermolecular interaction occurs in solution and taking into account the mixing entropy [24], the observed magnetic behavior of Fe^{II} allows the evaluation of the spin-crossover constant K_{sc} according to *Eqn. 7* [24], where x_{hs} is the mole fraction of high-spin Fe^{II} at temperature T, and μ_{hs} and μ_{ls} are the effective magnetic moments for the high- and low-spin forms, 5.0 and 0.3 BM, respectively [44].

$$K_{sc}(T) = \frac{x_{hs}}{1 - x_{hs}} = \frac{\mu_{eff}^2 - \mu_{ls}^2}{\mu_{hs}^2 - \mu_{eff}^2} \tag{7}$$

The calculated mole fractions x_{hs} evidence a smooth and incomplete spin transition in the temperature range 243–333 K (*Fig. 7b*): Fe^{II} is almost completely low-spin at 243 K, but *ca.* 40% high-spin at 333 K. The thermodynamic parameters ΔH_{sc} and ΔS_{sc} (*Table 7*) are estimated from plots of $\ln(K_{sc})$ *vs.* $1/T$ which are linear (correlation coefficients between 0.9905 and 0.9986). The values of ΔH_{sc} and ΔS_{sc} (*Eqn. 5*) for $[LnFe(L^2)_3]^{5+}$ are similar to those found for the $^1A \rightleftarrows {}^5T$ spin crossover in $[Fe(L^8)_3]^{2+}$ ($\Delta H_{sc} = 19.7(4)$ kJ·mol^{-1} and $\Delta S_{sc} = 78(2)$ J·mol^{-1}·K^{-1} in acetone and $\Delta H_{sc} = 21.4(1.6)$ kJ·mol^{-1} and $\Delta S_{sc} = 92(7)$ J·mol^{-1}·K^{-1} in MeCN/MeOH [16]) and for other $[Fe(diimine)_3]^{2+}$ complexes [15] [30]. ΔH_{sc} qualitatively reflects the changes in the metal-ligand bond distances and energies which occur upon conversion from low-spin to high-spin Fe^{II}. The inner-sphere reorganization energy associated with the elongation of the Fe–N bonds (0.11–0.24 Å) when going from low-spin to high-spin [24] [44] is expected to be 8 to 25 kJ·mol^{-1} [45] and to provide the dominant enthalpic contribution to these systems. The entropic factor ΔS_{sc} contains a relatively small electronic contribution associated with the degeneracy of the low- and high-spin states (22.5 J·mol^{-1}·K^{-1} for pure O_h symmetry, 13.4 J·mol^{-1}·K^{-1} for orbitally nondegenerate complexes [29]). The major contributions to ΔS_{sc} probably arise from vibrational partition functions since the disorder of the high-spin state is more pronounced owing to the longer metal–ligand bond length [24] [44]. In solution, outer-

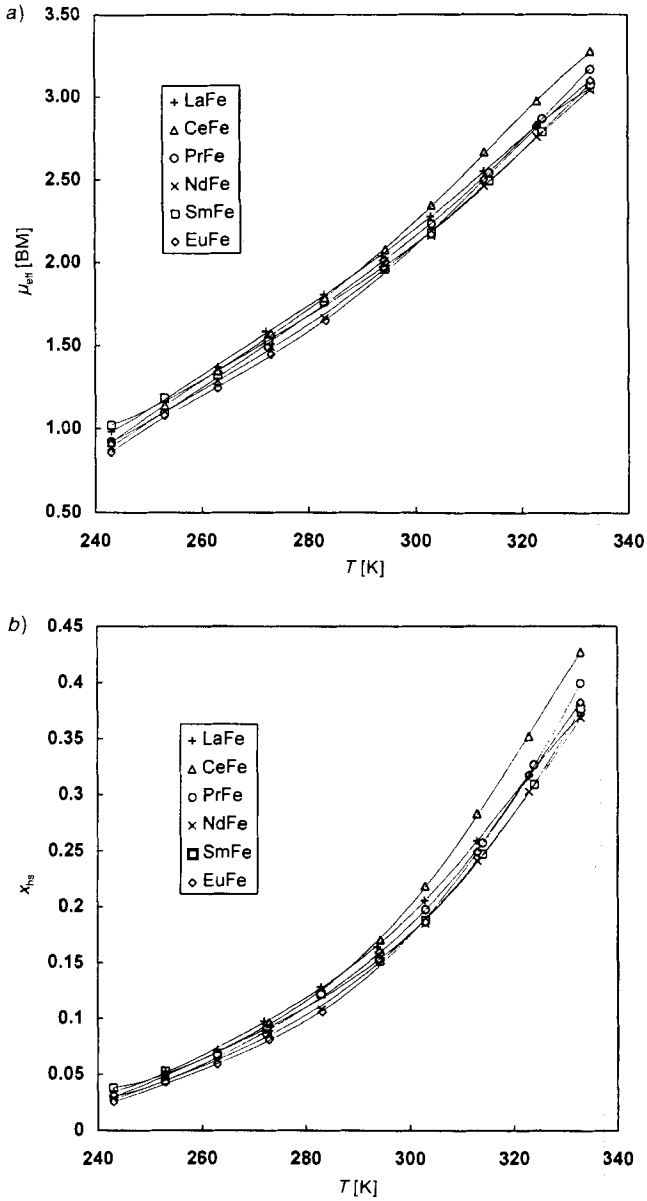

Fig. 7. a) *Effective magnetic moments of* Fe^{II} *and* b) *mole fraction of high-spin* Fe^{II} *in* $[LnFe(\mathbf{L}^2)_3]^{5+}$ (Ln = La–Eu) *in MeCN*

sphere reorganization of the solvent cage [16] may also significantly contribute to ΔS_{sc}. For $[LnFe(\mathbf{L}^2)_3]^{5+}$, ΔH_{sc} and ΔS_{sc} are similar for all the Ln^{III} studied (La–Eu), *i.e.*, the contraction of the ionic radii of Ln^{III} does not strongly affect the coordination sphere around Fe^{II} and the spin crossover is closely related to the coordination of Fe^{II} by the three bidentate units since $[Fe(\mathbf{L}^2)_2]^{2+}$ is diamagnetic.

Table 7. *Thermodynamic Parameter for* $^1A \rightleftarrows {}^5T$ *Spin-State Equilibria of* $[LnFe(L^2)_3](ClO_4)_5$ *in MeCN Obtained from Magnetic Measurements*

	ΔH_{sc} [kJ·mol^{-1}]	ΔS_{sc} [J·mol^{-1}·K^{-1}]	T_c [K][a])	σ[b])
$[LaFe(L^2)_3]^{5+}$	20.6(6)	57(3)	361	0.9986
$[CeFe(L^2)_3]^{5+}$	23.1(8)	66(4)	350	0.9966
$[PrFe(L^2)_3]^{5+}$	22.2(8)	62(3)	358	0.9960
$[NdFe(L^2)_3]^{5+}$	21.8(8)	60(3)	363	0.9968
$[SmFe(L^2)_3]^{5+}$	20.0(9)	55(4)	364	0.9905
$[EuFe(L^2)_3]^{5+}$	23.0(9)	64(3)	359	0.9955

[a]) Critical temperature for which $x_{hs} = 0.5$ ($T_c = \Delta H_{sc}/\Delta S_{sc}$) [24].
[b]) Correlation coefficients for plots of $Ln(K_{sc})$ *vs.* $1/T$ (see text).

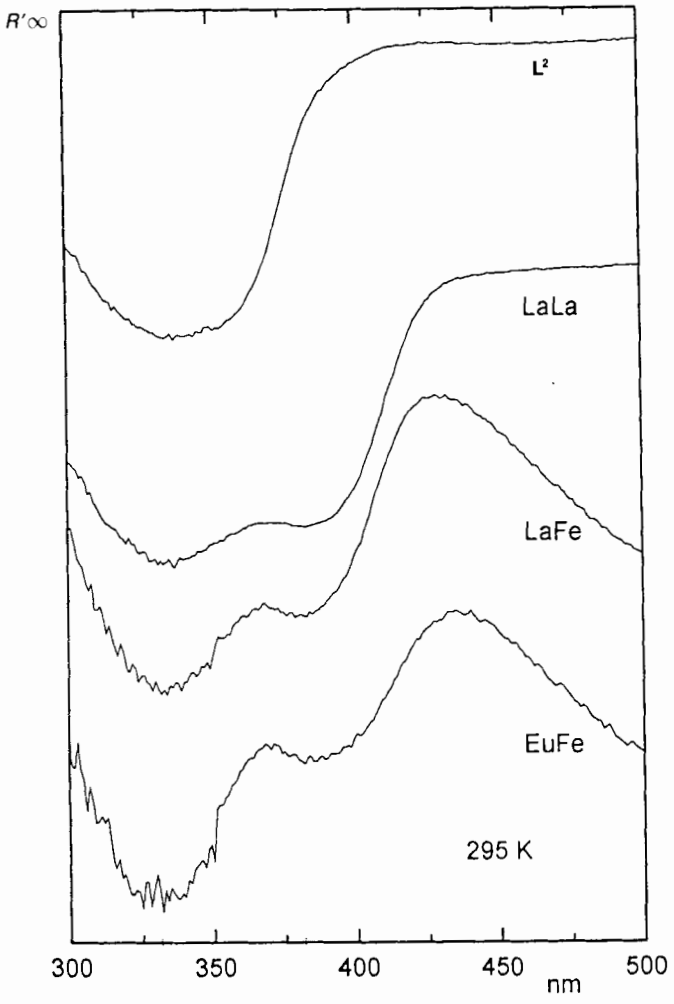

Fig. 8. *Reflectance spectra* (293 K) *of the ligand* L^2 *and its* $[La_2(L^2)_3]^{5+}$ [10] *and* $[LnFe(L^2)_3]^{5+}$ *complexes* (5% dispersion in MgO, reference: MgO)

Plots of the molar extinction (ε_{tot}) measured for the complexes $[LnFe(\mathbf{L}^2)_3]^{5+}$ (Ln = La, Nd, Eu) at different temperatures (*Fig. 4*) *vs.* calculated mole fractions x_{hs} given in *Table 6* allow the estimation of the molar extinction coefficients for the pure low-spin (ε_{ls}) and high-spin (ε_{hs}) complexes:

$$\varepsilon^{\lambda}_{tot} = \varepsilon^{\lambda}_{ls} - x_{hs}(\varepsilon^{\lambda}_{ls} - \varepsilon^{\lambda}_{hs}) \quad (8)$$

Straight lines are observed for the three complexes and molar extinction coefficients at the maximum of the MLCT band envelope (*ca.* 19000 cm^{-1}, *Table 2*) around 6000 $M^{-1} \cdot cm^{-1}$ are found for the low-spin form (ε_{ls} = 6000(200), 5800(200), and 5900(180) $M^{-1} \cdot cm^{-1}$ for Ln = La, Nd, and Eu, resp.), while the high-spin Fe^{II} form displays a much weaker absorption at the same wavelength (ε_{hs} = 480(90), 460(100), and 740(180) $M^{-1} \cdot cm^{-1}$ for Ln = La, Nd, and Eu, resp.), in good agreement with the values reported for $[Fe(\mathbf{L}^8)_3]^{2+}$ [16].

In the solid state, SQUID measurements of $[LaFe(\mathbf{L}^2)_3](ClO_4)_5 \cdot 8\ H_2O$ (**1**) show that the molar magnetic susceptibility corrected for paramagnetic impurities (*ca.* 2–3% Fe^{III}), and diamagnetism is almost temperature-independent in the range 100–310 K and corresponds to diamagnetic low-spin Fe^{II}. Above 310 K, the magnetic susceptibility slightly increases but the crystals readily decompose around 340 K which prevents the study at higher temperatures.

Photophysical Properties of $[LnFe(\mathbf{L}^2)_3](ClO_4)_5 \cdot 8\ H_2O$ (Ln = La, **1**; Ln = Eu, **3**) *in the Solid State.* Upon complexation, the splitting of the $\pi \rightarrow \pi^*$ transitions arising from the two nucleating parts of $\mathbf{L}^2$ (1000 cm^{-1} in the solid state [10]) increases to *ca.* 3400 cm^{-1} for $[LaFe(\mathbf{L}^2)_3]^{5+}$ and to *ca.* 4200 cm^{-1} for $[EuFe(\mathbf{L}^2)_3]^{5+}$ (*Fig. 8*), as in the analogous Zn^{II} compounds, revealing a structural similarity between the two series of compounds. Excitation of **1** in the UV (290, 308, and 340 nm) results in an extremely weak luminescence from the ligand with maxima around 23000 cm^{-1} ($^1\pi\pi^*$ state) and 19000 cm^{-1} ($^3\pi\pi^*$ state). No lifetime could be measured due to the efficient quenching occurring when Zn^{II} is replaced by Fe^{II}. The origin of the quenching most probably lies in the mixing with the MLCT state whose energy is very close to that of the ligand triplet state; additional mixing may also occur with the d-orbital states. The Eu-containing complex is still less luminescent, and no emission from the $Eu(^5D_0)$ state could be detected. This means that some ligand-to-europium energy transfer occurs, increasing the ligand quenching, but, in turn, the Eu luminescence is quenched by the MLCT state, resulting in an essentially non-luminescent compound.

Conclusion. – Zn^{II} and Fe^{II} display similar structural behaviors and lead to the selective thermodynamic [46] formation of the heterodinuclear C_3-cylindrical complexes $[LnZn(\mathbf{L}^2)_3]^{5+}$ and $[LnFe(\mathbf{L}^2)_3]^{5+}$ in solution (Ln = La–Eu), where the d-block metal ion occupies the pseudo-octahedral capping site defined by the three bidentate units and Ln^{III} lies in the resulting facial pseudo-tricapped trigonal prismatic site produced by the three tridentate binding units. Although the formation of the heterodinuclear complexes $[LnZn(\mathbf{L}^2)_3]^{5+}$ is observed along the complete lanthanide series (La–Lu) [10], $[LnFe(\mathbf{L}^2)_3]^{5+}$ may be only obtained with the larger Ln^{III} ions (La–Eu). A similar behavior occurs with ligands $\mathbf{L}^5$ and $\mathbf{L}^6$ for which mononuclear triple-helical $[Ln(\mathbf{L}^n)_3]^{3+}$ complexes are only obtained with the larger Ln^{III} ions [7] [9]. Structural factors limiting the rearrangements required for the coordination of the smaller Ln^{III} ions have been invoked [7], and the

origin of this promising size discriminating effect is currently under investigation [47]. For $[LnFe(L^2)_3]^{5+}$, the sterically more demanding Fe^{II}, as compared to Zn^{II}, probably distorts the structure and prevents the contraction required for the complexation of the smaller Ln^{III} ions in the heterodinuclear edifices. If we now consider the spectroscopic and magnetic properties of the complexes, $[LnFe(L^2)_3]^{5+}$ are complementary to $[LnZn(L^2)_3]^{5+}$ for structural investigation. The Zn^{II} complexes allow the study of the lanthanide coordination sites by using Ln^{III} as luminescent probes and ^{1}H-NMR paramagnetic shift reagents [10], while the Fe^{II} compounds allow the characterization of the pseudo-octahedral site occupied by the divalent metal ion which acts as a magnetic and spectroscopic probe. During the assembly process of L^2 with Ln^{III} and Fe^{II}, the transformation of $[Fe(L^2)_2]^{2+}$ into $[LnFe(L^2)_3]^{5+}$ may be monitored by the appearance of a red color and a spin-state equilibrium resulting from the shift of Fe^{II} from the tridentate to the bidentate units. The use of Fe^{II} as a probe is particularly appropriate for the investigation of the La^{III} complexes, since the formation of the spin-crossover complex $[LaFe(L^2)_3]^{5+}$ is easily characterized, while $[LaZn(L^2)_3]^{5+}$ is spectroscopically difficult to distinguish from its mononuclear precursor $[Zn(L^2)_2]^{2+}$ [10]. Detailed magnetic investigations of the heterodinuclear complexes $[LnFe(L^2)_3]^{5+}$ in MeCN show that the spin-state equilibrium $^1A \rightleftarrows {}^5T$ corresponds to a general feature of these compounds, since the associated thermodynamic parameters do not display significant variations with Ln(La–Eu).

In conclusion, the divalent d-block metal ions play a crucial structural role in the C_3-heterodinuclear $[LnM(L^2)_3]^{5+}$ complexes, leading to controlled C_3 'facial' tricapped trigonal prismatic coordination sites suitable for the coordination of lanthanide ions. A judicious choice of the d-metal ions, henceforth of its spectroscopic and magnetic properties, contributes to the elucidation of the final structure and to the control of intramolecular energy-transfer processes between the metal ions. This new efficient combination of structural magnetic and spectroscopic probes for the control and the investigation of heterodinuclear d–f complexes offers promising possibilities for the design of new organized molecular and supramolecular luminescent and magnetic materials containing lanthanide ions.

We gratefully acknowledge Ms. *Véronique Foiret* and Mr. *Bernard Bocquet* for their technical assistance. SQUID Measurements were performed by Prof. *J.-P. Ansermet*, Swiss Federal Institute of Technology, Lausanne. We are grateful to Prof. *A. Williams*, University of Geneva, for helpful comments. *J.-C. B.* thanks the *Fondation Herbette*, Lausanne, for the gift of spectroscopic equipment. This work is supported through grants from the *Swiss National Science Foundation*.

Experimental Part

General. See [10b].

Tris{2-{6-[1-(3,5-dimethoxybenzyl)-1H-benzimidazol-2-yl]pyridin-2-yl}-1,1'-dimethyl-5,5'-methylene-2'-(5-methylpyridin-2-yl)bis[1H-benzimidazole]}iron(II)lanthanide(III) Pentaperchlorate – Water (1/8) ($[LnFe(L^2)_3](ClO_4)_5 \cdot 8\,H_2O$ (Ln = La, **1**; Nd, **2**; Ln = Eu, **3**). A soln. of $2.34 \cdot 10^{-2}$ mmol of $Ln(ClO)_4)_3 \cdot n\,H_2O$ (Ln = La, Nd, Eu; n = 6–8) and 8.5 mg ($2.34 \cdot 10^{-2}$ mmol) of $Fe(ClO_4)_2 \cdot 6\,H_2O$ in MeCN (5 ml) was slowly added to 50 mg ($7.04 \cdot 10^{-2}$ mmol) of *2-{6-[1-(3,5-dimethoxybenzyl)-1H-benzimidazol-2-yl]pyridin-2-yl}-1,1'-dimethyl-5,5'-methylene-2'-(5-methylpyridin-2-yl)bis[1H-benzimidazole]* (L^2) [48] in 10 ml of CH_2Cl_2/MeCN 1:1. After stirring for 2 h at r.t., the soln. was evaporated, the solid residue dissolved in MeCN and Et_2O was slowly diffused into the soln. for 2–3 days. The resulting deep red precipitate was collected by filtration and dried to give 83–94% of **1** (Ln = La), **2** (Ln = Nd), or **3** (Ln = Eu).

1: Anal. calc. for $C_{132}H_{114}Cl_5FeLaN_{24}O_{26}\cdot 8\,H_2O$: C 53.4, H 4.4, Fe 1.9, La 4.7, N 11.3; found: C 53.7, H 4.6, Fe 2.1, La 4.8, N 11.3.

2: Anal. calc. for $C_{132}H_{114}Cl_5FeN_{24}NdO_{26}\cdot 8\,H_2O$: C 53.3, H 4.4, Fe 1.9, N 11.3, Nd 4.9; found: C 53.7, H 4.3, Fe 2.0, N 11.1, Nd 4.9.

3: Anal. calc. for $C_{132}H_{114}Cl_5EuFeN_{24}O_{26}\cdot 8\,H_2O$: C 53.2, H 4.4, Eu 5.1, Fe 1.9, N 11.3; found: C 53.5, H 4.5, Eu 5.3, Fe 2.2, N 11.2.

For IR spectra, elemental analyses (C,H,N), and metal content, see [10b].

In situ *Preparation of [LnFe(L^2)$_3$](ClO$_4$)$_5$* (Ln = Ce, Pr, Sm, Y) *for ^{1}H-NMR and Magnetic Studies.* A 10^{-2} M soln. of $Ln(ClO_4)_3\cdot nH_2O$ and $Fe(ClO_4)_2\cdot 6\,H_2O$ in MeCN (263 µl, $5.26\cdot 10^{-3}$ mmol) was added to 11.2 mg ($1.58\cdot 10^{-2}$ mmol) of L^2 dissolved in 5 ml of CH_2Cl_2/MeCN 1:1. After evaporation of the soln., the solid residue was dried under vacuum and dissolved in 700 µl of degassed CD_3CN to give a $7.5\cdot 10^{-3}$ M soln. of $[LnFe(L^2)_3](ClO_4)_5$ (Ln = Ce, Pr, Sm) whose purity was checked by ^{1}H-NMR spectroscopy.

Caution! Perchlorate salts combined with org. ligands are potentially explosive and should be handled with the necessary precautions [49].

Spectroscopic Measurements. Reflectance, IR, pneumatically-assisted electrospray (ES) mass, and ^{1}H-NMR spectra, as well as spectrophotometric titrations were recorded as described in [10].

Magnetic Measurements. Magnetic data for samples in MeCN were obtained by *Evans'* method [18] using a *Varian-Gemini-300* spectrometer. The method was modified according to *Baker et al.* [37] for application with a superconducting magnet. Measurements were carried out on degassed solns. containing $7.5\cdot 10^{-3}$ M of complex and 1% (v/v) of $SiMe_4$ as an internal reference. All the data were corrected for diamagnetism as follows. The contributions of the ligand L^2 and of the perchlorate anions in the heterodinuclear complexes $[LnFe(L^2)_3](ClO_4)_5$ were obtained from the molar susceptibility measured for $[YZn(L^2)_3](ClO_4)_5$ according to the procedure described by *Linert et al.* [14]. The molar susceptibility $\chi_d([YZn(L^2)_3](ClO_4)_5)$ amounts to $-1910(60)\cdot 10^{-6}$ cm$^3\cdot$mol^{-1} at 294 K for a total ligand concentration of 0.02M. It deviates significantly from that derived from *Pascal* constants (*ca.* $-1300\cdot 10^{-6}$ cm$^3\cdot$mol^{-1}) but is consistent with the experimental value found for L^2, $\chi_d = -690(50)\cdot 10^{-6}$ cm$^3\cdot$mol^{-1} using the same method. Molar magnetic susceptibilities of $[LnFe(L^2)_3](ClO_4)_5$ were then measured at 10-K intervals between 243 and 333 K, corrected for diamagnetism and converted to effective magnetic moments μ_{eff} [25] according to *Eqn. 9* [37] where c is the concentration of the paramagnetic solute (g$\cdot$ml^{-1}), $\Delta\nu$ the chemical-shift difference (Hz) between the resonances of the reference compound in the two coaxial tubes [18] ($\Delta\nu > 0$ for paramagnetism, $\Delta\nu < 0$ for diamagnetism), ν the operating frequency of the NMR spectrometer (Hz), χ_0 the mass susceptibility of the solvent (cm$^3\cdot$g^{-1}), χ_d the molar diamagnetic susceptibility of the paramagnetic compound (cm$^3\cdot$mol^{-1}), M the molecular weight of the paramagnetic compound (g$\cdot$mol^{-1}), T the absolute temperature, μ_{eff} the effective magnetic moment (BM), and S_f the shape factor of the magnet: $4\pi/3$ for a superconducting magnet (χ_0 and χ_d are negative) [37].

$$\mu_{eff} = 2.828\cdot\sqrt{\frac{T\cdot M}{S_f\cdot c}\left(\frac{\Delta\nu}{\nu} + S_f\cdot c\cdot\chi_0 - \frac{S_f\cdot c}{MW}\cdot\chi_d\right)} \qquad (9)$$

To check for complications associated with possible partial decomplexation [14], the magnetic susceptibilities of $[LnFe(L^2)_3](ClO_4)_5$ (Ln = La, Eu) were recorded for total ligand concentrations between 1.5 and $2.5\cdot 10^{-2}$ M at each temp. (243–333 K). No significant variation of μ_{eff} was observed within experimental error, which confirms the ^{1}H-NMR data and demonstrates that $[LnFe(L^2)_3]^{5+}$ (Ln = La, Eu) are the only species formed in solution. All subsequent magnetic measurements were obtained from $7.5\cdot 10^{-3}$ M solns. with a total ligand concentration equal to $2.25\cdot 10^{-2}$ M.

Electrochemical Measurements. Cyclic voltammograms were recorded using a *BAS-CV-50W* potentiostat connected to a personal computer. A three-electrode system consisting of a stationary Pt-disk working electrode, a Pt counter electrode and a nonaqueous Ag/AgCl reference electrode was used. $(Bu_4N)PF_6$ (0.1M in MeCN) served as an inert electrolyte. MeCN was distilled from P_2O_5 and then passed through an alumina column (act. I). The reference potential ($E^0 = -0.12$ V *vs.* SCE) was standardized against $[Ru(bipy)_3](ClO_4)_2$ [50]. The scan speed used was 100 mV/s, and voltammograms were analyzed according to established procedures [50].

REFERENCES

[1] J.-C.G. Bünzli, P. Froidevaux, J. MacB. Harrowfield, *Inorg. Chem.* **1993,** *32,* 3306; P. Guerriero, P.A. Vigato, J.-C.G. Bünzli, E. Moret, *J. Chem. Soc., Dalton Trans.* **1990,** 647; G. Denti, S. Serroni, S. Campagna, A. Juris, M. Ciano, V. Balzani, in 'Perspectives in Coordination Chemistry', Eds. A.F. Williams, C. Floriani, and A.E. Merbach, VHCA, Basel, 1992, p.153; Z. Pikramenou, Y. Yu, R.B. Lessard, A. Ponce, P.A. Wong, D.G. Nocera, *Coord. Chem. Rev.* **1994,** *132,* 181; F. Barigelletti, L. Flamigni, V. Balzani, J.-P. Collin, J.-P. Sauvage, A. Sour, E.C. Constable, A.M.W. Cargill-Thompson, *ibid.* **1994,** *132,* 209; D. Gust, T.A. Moore, A.L. Moore, A.N. McPherson, A. Lopez, J.M. De Graziano, I. Gouni, E. Bittersmann, G.R. Seely, F. Gao, R.A. Nieman, X.C. Ma, L.J. Demanche, S.C. Hung, D.K. Luttrull, S.J. Lee, P.K. Kerrigan, *J. Am. Chem. Soc.* **1993,** *115,* 11141.

[2] J.-C. Chambron, V. Heitz, J.-P. Sauvage, *J. Am. Chem. Soc.* **1993,** *115,* 12378; J.-P. Sauvage, J.-P. Collin, J.-C. Chambron, S. Guillerez, C. Coudret, V. Balzani, F. Barigelletti, L. De Cola, L. Flamigni, *Chem. Rev.* **1994,** *94,* 993.

[3] J.-C.G. Bünzli, in 'Lanthanide Probes in Life, Chemical and Earth Sciences', Eds. J.-C.G. Bünzli and G.R. Choppin, Elsevier Science Publ., Amsterdam, 1989, Chapt. 7; F.S. Richardson, *Chem. Rev.* **1982,** *82,* 541.

[4] G.R. Choppin, in 'Lanthanide Probes in Life, Chemical and Earth Sciences', Eds. J.-C.G. Bünzli and G.R. Choppin, Elsevier Science Publ., Amsterdam, 1989, Chapt. 1.

[5] N. Sabbatini, M. Guardigli, J.-M. Lehn, *Coord. Chem. Rev.* **1993,** *123,* 201.

[6] R. Ziessel, M. Maestri, L. Prodi, V. Balzani, A. Van Doersselaer, *Inorg. Chem.* **1993,** *32,* 1237; N. Sabbatini, M. Guardigli, I. Manet, F. Bolleta, R. Ziessel, *ibid.* **1994,** *33,* 955; N. Sabbatini, M. Guardigli, I. Manet, R. Ungaro, A. Casnati, C. Fischer, R. Ziessel, G. Ulrich, *New J. Chem.* **1995,** *19,* 137.

[7] C. Piguet, J.-C.G. Bünzli, G. Bernardinelli, A.F. Williams, *Inorg. Chem.* **1993,** *32,* 4139.

[8] C. Piguet, J.-C.G. Bünzli, G. Bernardinelli, G. Hopfgartner, A.F. Williams, *J. Am. Chem. Soc.* **1993,** *115,* 8197.

[9] C. Piguet, J.-C.G. Bünzli, G. Bernardinelli, C.G. Bochet, P. Froidevaux, *J. Chem. Soc., Dalton Trans.* **1995,** 83.

[10] a) C. Piguet, G. Hopfgartner, A.F. Williams, J.-C.G. Bünzli, *J. Chem. Soc., Chem. Commun.* **1995,** 491; b) C. Piguet, E. Rivara-Minten, G. Hopfgartner, J.-C.G. Bünzli, *Helv. Chim. Acta* **1995,** *78,* 1541.

[11] C.G. Bochet, C. Piguet, A.F. Williams, *Helv. Chim. Acta* **1992,** *75,* 1697.

[12] C. Piguet, G. Hopfgartner, B. Bocquet, O. Schaad, A.F. Williams, *J. Am. Chem. Soc.* **1994,** *116,* 9092; C. Piguet, G. Bernardinelli, A.F. Williams, B. Bocquet, *Angew. Chem. Int. Ed.* **1995,** *34,* 582.

[13] A.W. Addison, S. Burman, C.G. Wahlgren, O.A. Rajan, T.M. Rowe, E. Sinn, *J. Chem. Soc., Dalton Trans.* **1987,** 2621; S. Rüttimann, C.M. Moreau, A.F. Williams, G. Bernardinelli, A.W. Addison, *Polyhedron* **1992,** *11,* 635.

[14] W. Linert, M. Konecny, F. Renz, *J. Chem. Soc., Dalton Trans.* **1994,** 1523.

[15] H. Toftlund, *Coord. Chem. Rev.* **1989,** *94,* 67.

[16] K.A. Reeder, E.V. Dose, L.J. Wilson, *Inorg. Chem.* **1978,** *17,* 1071.

[17] D.H. Metcalf, J.M.McD. Stewart, S.W. Snyder, C.M. Grisham, F.S. Richardson, *Inorg. Chem.* **1992,** *31,* 2445; D.H. Metcalf, J.-P. Bolender, M.S. Driver, F.S. Richardson, *J. Phys. Chem.* **1993,** *97,* 553; P.A. Brayshaw, J.-C.G. Bünzli, P. Froidevaux, J.M. Harrowfield, Y. Kim, A.N. Sobolev, *Inorg. Chem.* **1995,** *34,* 2068.

[18] D.F. Evans, *J. Chem. Soc.* **1959,** 2037; T.H. Crawford, J. Swanson, *J. Chem. Educ.* **1971,** *48,* 382; J. Löliger, R. Scheffold, *ibid.* **1972,** *49,* 646; D.H. Grant, *ibid.* **1995,** *72,* 39.

[19] G. Hopfgartner, C. Piguet, J.D. Henion, A.F. Williams, *Helv. Chim. Acta* **1993,** *76,* 1759; G. Hopfgartner, C. Piguet, J.D. Henion, *J. Am. Chem. Soc. Mass Spectrom.* **1994,** *5,* 748.

[20] E.R. Malinowski, D.G. Howery, 'Factor Analysis in Chemistry', Wiley, New York, 1980.

[21] P. Krumholz, Structure and Bonding, Springer Verlag, Berlin–Heidelberg–New York, 1971, Vol. 9, p. 139.

[22] S. Rüttimann, C. Piguet, G. Bernardinelli, B. Bocquet, A.F. Williams, *J. Am. Chem. Soc.* **1992,** *114,* 4230.

[23] D.K. Lavallee, M.D. Baughman, M.P. Phillips, *J. Am. Chem. Soc.* **1977,** *99,* 718.

[24] O. Kahn, 'Molecular Magnetism', VCH Publishers Inc., Weinheim, 1993.

[25] B.N. Figgis, J. Lewis, in 'Modern Coordination Chemistry', Interscience Publishers Inc., New York, 1960, p.400.

[26] D. Onggo, H.A. Goodwin, *Aust. J. Chem.* **1991,** *44,* 1539.

[27] K.F. Purcell, J.C. Kotz, 'Inorganic Chemistry', W.B. Saunders Comp., Philadelphia–London–Toronto, 1987, p.717.

[28] P.W. Jensen, L.B. Jorgensen, *J. Mol. Struct.* **1982,** *79,* 87.
[29] P. Gütlich, A. Hauser, H. Spiering, *Angew. Chem. Int. Ed.* **1994,** *33,* 2024.
[30] K.H. Sugiyarto, D.C. Craig, A.D. Rae, H.A. Goodwin, *Aust. J. Chem.* **1995,** *48,* 35.
[31] P.D. Burns, G.N. La Mar, *J. Magn. Reson.* **1982,** *46,* 61.
[32] C.N. Reilley, B.W. Good, J.F. Desreux, *Anal. Chem.* **1975,** *47,* 2111.
[33] I. Bertini, C. Luchinat, 'NMR of Paramagnetic Molecules in Biological Systems', Benjamin/Cummings Publishing Co., Inc., 1986.
[34] R.D. Shannon, *Acta Crystallogr., Sect. A* **1976,** *32,* 751.
[35] M.-T. Youinou, R. Ziessel, J.-M. Lehn, *Inorg. Chem.* **1991,** *30,* 2144.
[36] P.S. Braterman, J.I. Song, R.D. Peacock, *Inorg. Chem.* **1992,** *31,* 555.
[37] M.V. Baker, L.D. Field, T.W. Hambley, *Inorg. Chem.* **1988,** *27,* 2872.
[38] I. Morgenstein-Badarou, D. Cocco, A. Desideri, G. Rotilio, J. Jordanov, N. Dupré, *J. Am. Chem. Soc.* **1986,** *108,* 300.
[39] A. Bouayad, C. Brouca-Cabarrecq, J.-C. Trombe, *Inorg. Chim. Acta* **1992,** *195,* 193; C. Benelli, A. Caneschi, D. Gatteschi, O. Guillou, L. Prodi, *Inorg. Chem.* **1990,** *29,* 1750.
[40] M. Sakamoto, M. Hashimura, K. Matsuki, N. Matsumoto, K. Inoue, H. Okawa, *Bull. Chem. Soc. Jpn.* **1991,** *64,* 3639; M. Andruh, I. Ramade, E. Codjovi, O. Guillou, O. Kahn, J.-C. Trombe, *J. Am. Chem. Soc.* **1993,** *115,* 1822; Y.-T. Li, Z.-H. Jiang, D.-Z. Liao, S.-P. Yan, S.-L. Ma, X.-Y. Li, G.L. Wang, *Polyhedron* **1993,** *12,* 2785.
[41] G. Bernardinelli, C. Piguet, A.F. Williams, *Angew. Chem. Int. Ed.* **1992,** *12,* 1622.
[42] C. Piguet, G. Bernardinelli, B. Bocquet, O. Schaad, A.F. Williams, *Inorg. Chem.* **1994,** *33,* 4112.
[43] L. Chen, S.R. Breeze, R.J. Rousseau, S. Wang, L.K. Thompson, *Inorg. Chem.* **1995,** *34,* 454.
[44] K.H. Sugiyarto, D.C. Craig, D.A. Rae, H.A. Goodwin, *Aust. J. Chem.* **1994,** *47,* 869.
[45] E.V. Dose, M.A. Hoselton, N. Sutin, M.F. Tweedle, L.J. Wilson, *J. Am. Chem. Soc.* **1978,** *100,* 1141; R.H. Petty, E.V. Dose, M.F. Tweedle, L.J. Wilson, *Inorg. Chem.* **1978,** *17,* 1064.
[46] A.F. Williams, C. Piguet, R. Carina, in 'Transition Metals in Supramolecular Chemistry', Eds. L. Fabbrizzi and A. Poggi, Kluwer Academic Publishers, Dordrecht–Boston–London, 1994, Vol. 448, p. 409–424.
[47] S. Petoud, J.-C.G. Bünzli, C. Piguet, unpublished results.
[48] C. Piguet, B. Bocquet, G. Hopfgartner, *Helv. Chim. Acta* **1994,** *77,* 931.
[49] W.C. Wolsey, *J. Chem. Educ.* **1978,** *55,* A355.
[50] A.J. Bard, L.R. Faulkner, 'Electrochemical Methods, Fundamentals and Applications', J. Wiley, New York–Chichester–Brisbane–Toronto–Singapore, 1980.